Calculated magneto-optical Kerr spectra of XPt_3 compounds (X = V, Cr, Mn, Fe and Co)

1996 J. Phys.: Condens. Matter 8 5769

(http://iopscience.iop.org/0953-8984/8/31/010)

J. Phys.: Condens. Matter **8** (1996) 5769–5780. Printed in the UK

Calculated magneto-optical Kerr spectra of XPt_3 compounds (X = V, Cr, Mn, Fe and Co)

P M Oppeneer†, V N Antonov‡, T Kraft†, H Eschrig†, A N Yaresko‡ and A Ya Perlov‡

† Max-Planck Research Group 'Theory of Complex and Correlated Electron Systems', University of Technology, D-01062 Dresden, Germany

‡ Institute of Metal Physics, Academy of Science of Ukraine, 252680, Kiev, Ukraine

Received 9 May 1996

Abstract. The magneto-optical spectra of the XPt_3 compounds (with X = V, Cr, Mn, Fe and Co) are calculated for their ferromagnetic phase in the $AuCu_3$ crystal structure, using density-functional band-structure theory. Large polar Kerr effects are predicted for several of these compounds, with—for a reasonable spectral broadening of 0.4 eV—maximum Kerr rotations of -1.5° for $MnPt_3$ and -1.0°, -1.1° for $CoPt_3$ and $FePt_3$, respectively. The Kerr spectra of VPt_3, $CrPt_3$ and $MnPt_3$ with (001) magnetization are found to be very similar in shape, as are also those of $FePt_3$ and $CoPt_3$. The origin of the large Kerr effect in the XPt_3 alloys is shown to be caused by the spin–orbit coupling strength of Pt. A magnetic moment of moderate size on the 3d atom suffices in these materials to already create an appreciable Kerr effect. The influence of the optical transition matrix elements, magnetic moments and spin–orbit coupling strength on each of the constituent atoms are furthermore analysed. The orientation dependence of the polar Kerr spectra of some of the XPt_3 compounds are investigated by calculating in addition the polar Kerr spectra of some compounds for the (111) magnetization axis. The Kerr spectra of the (111) magnetization are found to be practically identical to that of the (001) magnetization.

1. Introduction

Transition-metal alloys, which consist of a ferromagnetic 3d element and Pt, have drawn attention over the last years because of their good magneto-optical (MO) properties (see e.g. [1–3]). In particular, multi-layers of Co and Pt or Pd are at present intensively studied because of their potential application as optical storage material in MO storage devices [4–6]. In addition to this, it has very recently been discovered that the compound $MnPt_3$ exhibits a very large MO Kerr rotation, of about -1.2° at 1 eV photon energy [7,8]. This discovery indicates, firstly, that the whole group of transition-metal-platinum alloys is exceptionally interesting for MO research, and secondly, that large Kerr effects might still be found in materials which were previously not regarded for their MO properties.

With the aim of undertaking a systematic investigation of the trends in transition-metal-platinum alloys, in the present work we study theoretically the MO Kerr spectra of the series XPt_3, with X = V, Cr, Mn, Fe and Co. The computational method used here is an evaluation of the MO spectra resulting from optical interband transitions between occupied and unoccupied energy bands based on the linear response formalism [9,10]. The energy-band structure and single-particle electron wave functions are calculated in the framework of the density-functional theory [11,12] in the local spin-density approximation (LSDA) [13]. This

0953-8984/96/315769+12$19.50

approach has been found to be very satisfactory for the description—and even prediction—of Kerr spectra of transition-metal compounds [14–19]. As a consequence, with the present state-of-the-art computational techniques, it is becoming feasible to undertake MO research and predict good MO materials by doing *ab initio* calculations of the Kerr spectra. An example of this development is the compound FePt, for which theory first predicted a large Kerr rotation, which was then subsequently measured on a good quality molecular-beam-epitaxy grown sample [20]. Prerequisite to obtaining any Kerr signal is the presence of a ferromagnetic (or ferrimagnetic) phase (see e.g. Reim and Schoenes [21]). In this respect, we mention that the XPt_3 compounds being examined in the present work do not all exist in a ferromagnetic ground state: $FePt_3$ was found to have an anti-ferromagnetic ground state [22]. In this case, the MO spectra calculated for the ferromagnetic state should correspond to those of $FePt_3$ in an applied magnetic field. All XPt_3 compounds investigated also have in common that they exist in the $AuCu_3$ crystal structure.

Apart from studying the trends in the MO spectra of the XPt_3 compounds, a second goal of the present work is to obtain a microscopic understanding of the physical quantities that give rise to large peaks in the Kerr rotation spectrum. To this end, we study the influence of the size of the magnetic moment on the 3d atom and on Pt, and the influence of the spin–orbit coupling on either of the two kinds of elements. In addition, we analyse the importance of the various allowed interband transitions by excluding the matrix elements of selected optical transitions. From studying this model we can then conclude which energy-band transitions on which atoms are responsible for peaks in the Kerr rotation spectrum. The obtained Kerr spectra are furthermore compared to the calculated band structure and total density of states. The orientation dependence of the Kerr spectra, finally, is examined by also computing the polar Kerr spectra pertaining to a magnetization oriented along the (111) axis for some compounds.

2. Results

In the so-called polar geometry, in which the magnetization and incident light wave vector are oriented perpendicular to the surface of the magnetic solid, the MO Kerr effect can be written in terms of the optical conductivity [23]

$$\theta_{\mathrm{K}}(\omega) + i\varepsilon_{\mathrm{K}}(\omega) = -\frac{\sigma_{xy}(\omega)}{\sigma_{xx}(\omega)}\left(1 + \frac{4\pi i}{\omega}\sigma_{xx}(\omega)\right)^{-1/2} \tag{1}$$

with θ_{K} the polar Kerr rotation angle, ε_{K} the polar Kerr ellipticity, and σ_{ij} are components of the optical conductivity tensor. The local z-direction is chosen here along the normal vector to the surface. The optical conductivity is known to consist of two contributions, the intraband and interband contribution. The intraband optical conductivity is caused by various Bloch electron scattering processes at the Fermi energy. Despite the inherent complexity of such processes, the intraband conductivity can, for most materials, be reasonably approximated by an empirical Drude conductivity [21]. It normally only contributes to the Kerr rotation at small photon frequencies. In the present work we shall therefore ignore the intraband part of the conductivity and consider only the interband spectra.

The *ab initio* evaluation of the full interband optical conductivity tensor is the computationally intensive task of the present study. We used here the computational scheme of Oppeneer *et al* [14], which is implemented on a relativistic version of the augmented-spherical-wave (ASW) band-structure method [24]. In addition, we also use a fully relativistic version [25] of the linear muffin-tin orbital (LMTO) method [26] together with a recently developed computational scheme for the MO spectra [27]. This offers us

the possibility of benefitting from the computational specialties inherent to the two schemes in studying the origin of peaks in the Kerr spectra. For instance, within the ASW method, where spin–orbit (SO) interaction is treated in a second variation, we can study the influence of SO coupling by scaling the SO term in the Hamiltonian with a prefactor. In the scheme based on the fully relativistic LMTO method, we study the importance of the exchange splitting by scaling the spin-polarized part of the potential in the Dirac equation. Both schemes yield identical results for the energy-band structure, and, as we showed before, also for the Kerr spectra [16].

The MO Kerr spectra are calculated here only for the chemical $AuCu_3$ unit cell. The thus obtained magnetic ground state can therefore be ferro-, ferri-, or paramagnetic, but not anti-ferromagnetic. Since an anti-ferromagnetic material is known to have a vanishing Kerr effect [21], it would thus be of no interest in the present investigation. This is of concern only for $FePt_3$, which is reported to have an anti-ferromagnetic ground state [22]. While it is certainly of interest to understand why $FePt_3$ has an anti-ferromagnetic ground state, whereas the other XPt_3 compounds and also $FePd_3$ have a ferro- (or ferri-) magnetic ground state, this is not the subject of the present investigation. For a recent discussion of the magnetic properties of $FePt_3$, we refer to Kaburagi *et al* [28]. The MO spectra of ferromagnetic $FePt_3$ caculated here corresponds therefore to $FePt_3$ in an applied magnetic field. All lattice constants of the XPt_3 alloys used are the experimental ones taken from the literature [29].

To start with, we show the calculated polar Kerr spectra of VPt_3, $CrPt_3$ and $MnPt_3$ in figure 1, and those of $FePt_3$ and $CoPt_3$ in figure 2. All Kerr spectra given in figures 1 and 2 pertain to the (001) magnetization direction, and, as we mentioned before, are due to the interband optical conductivity tensor only. A Lorentzian broadening with a half width at half maximum of 0.4 eV, taking account of the effects of finite lifetimes and of the experimental resolution, has been applied to all optical conductivity spectra [14]. In figure 1, the recently measured Kerr spectra of $MnPt_3$ are also shown [7]. As one can see from figures 1 and 2, the Kerr spectra of VPt_3, $CrPt_3$ and $MnPt_3$ are very similar, as are those of $FePt_3$ and $CoPt_3$. This is the reason why we show the spectra in this combination together. The theoretical Kerr rotations of VPt_3, $CrPt_3$ and $MnPt_3$ have their minimum at the same photon energy of 0.8 eV, followed by a zero crossing at 2 eV. This similarity is partially observed in the Kerr ellipticity too. The Kerr rotations of both $FePt_3$ and $CoPt_3$, however, are distinctly different, as they have no zero crossing, and exhibit two minima, one smaller minimum at 1.3 eV, and a larger one at 4.7 eV. Noticeable also, are the large Kerr rotations that are predicted by density-functional theory for these compounds. The largest Kerr rotation is found for $MnPt_3$, which reaches a value of -1.5° at 0.8 eV. But also the Kerr rotation of the as yet not investigated $CrPt_3$ alloy is surprisingly large, being with a peak value of -0.9° at 0.8 eV larger than that of the transition metals Fe and Co [30,31]. Additionally the Kerr rotations predicted for $FePt_3$ and $CoPt_3$ are also substantial with peak values of -1.0° to -1.1° at 4.7 eV. (The term 'peak' is commonly used for a maximal Kerr rotation, irrespective of whether it has a positive or negative sign.) With respect to the magnitudes of the Kerr rotations displayed in figures 1 and 2, there are three points to be mentioned. In the first place, the precise peak magnitude depends on the applied broadening parameter [14]. A larger broadening than 0.4 eV would generally lead to slightly smaller, but broader spectral peaks. However, so far it is our experience that the broadening parameter of 0.4 eV gives a physically adequate description [14–16]. Secondly, the neglect of the intraband contribution to the optical conductivity can play a role for VPt_3, $CrPt_3$ and $MnPt_3$. An intraband Drude contribution to the optical conductivity can be of importance for the Kerr rotation spectrum at small photon energies [14]. As the

main Kerr rotation peak of the compounds in figure 1 occurs at a small energy, the size of this peak will become reduced when a large intraband contribution is present. For $CoPt_3$ and $FePt_3$, the intraband contribution is less important, because these compounds already have a relatively small Kerr rotation at low energies (see figure 2). Thirdly, it should be noted that the *ab initio* Kerr spectra are essentially calculated for zero temperature. If the Kerr spectra are measured at room temperature, where the magnetization is reduced, then the overall size of the thus measured Kerr rotation will be reduced too. This property is further examined in more detail in section 3.

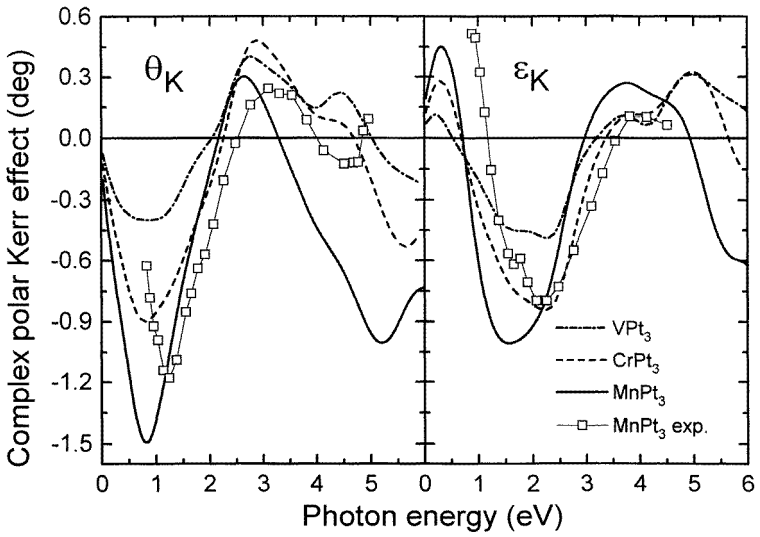

Figure 1. Calculated polar Kerr rotation (θ_K) and Kerr ellipticity (ε_K) spectra of VPt_3, $CrPt_3$, and $MnPt_3$ in the $AuCu_3$ crystal structure with (001) magnetization axis. The theoretical spectra are all calculated with a relaxation-time broadening of 0.4 eV, and result from the interband optical conductivity only. The experimental data shown are those of $MnPt_3$ [7].

In figure 1 the recently measured Kerr spectra of ordered $MnPt_3$ are also shown [7,8]. These spectra were measured from an annealed thin film of $MnPt_3$ on a quartz substrate, but from the substrate side, i.e., through quartz [7]. This implies that the thus measured spectra can be enhanced over the Kerr spectra measured in air by a factor of about one and a half. Within the limitations concerning the size of the Kerr rotation mentioned above, and the possible influence of the quartz substrate on the Kerr spectra, it can as yet only be concluded that the shape of the theoretical and experimental Kerr rotation and ellipticity spectra are in good agreement. In this respect we also mention that recent experiments on $MnPt_3$ films at 80 K [8] show that the Kerr rotation at low temperatures becomes enhanced over the room temperature result given in figure 1. In the case of $CoPt_3$, measurements of the Kerr spectra were recently made on a sample near the $CoPt_3$ composition [32], yielding a Kerr rotation spectrum that agrees very well in shape with an earlier *ab initio* calculation [32] (using the same computational scheme [14]), but the measured rotation was about 30% smaller than the calculated one. This difference was attributed to a reduction of the sample magnetization at room temperature [32].

The interband optical spectra originate from optical transitions between energy bands of the solid. To investigate the relationship between the optical spectra and the band structure, we show the energy bands and total density of states (DOS) of the XPt_3 compounds in

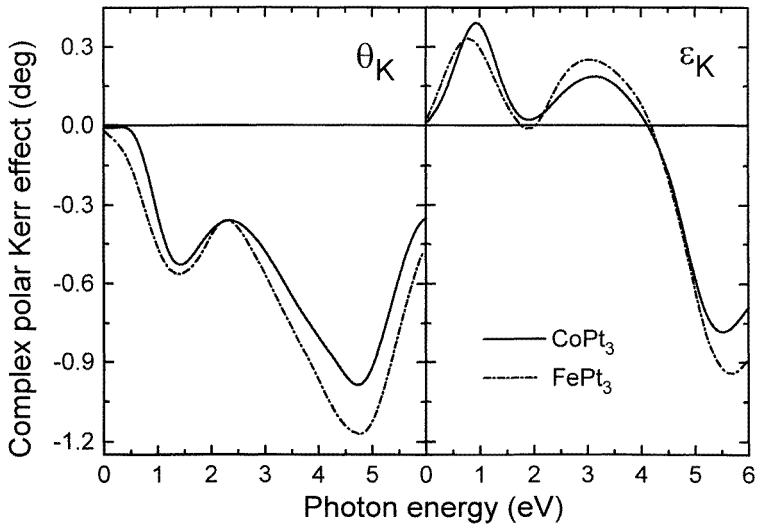

Figure 2. As figure 1, but for the theoretical polar Kerr spectra of $FePt_3$ and $CoPt_3$.

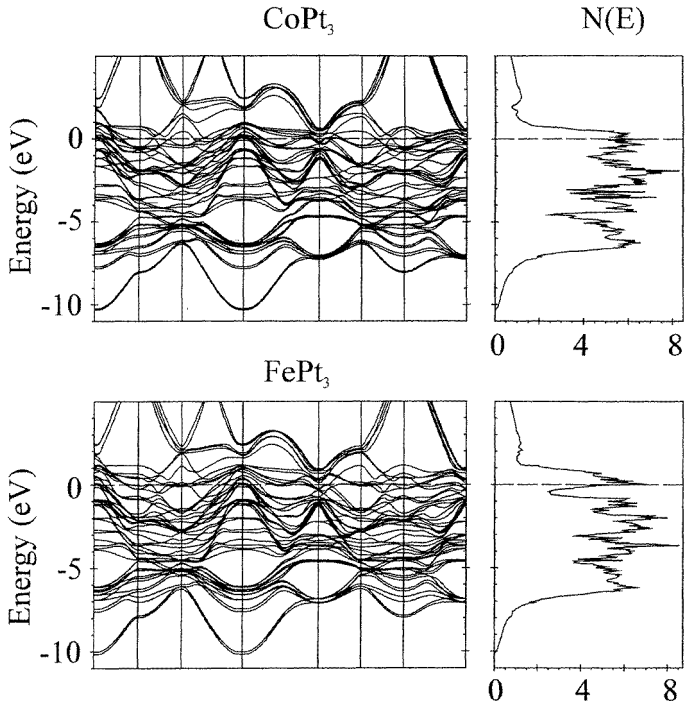

Figure 3. Relativistic band structure and total density of states (N(E)) for the XPt_3 alloys, with X = V, Cr, Mn, Fe and Co.

figure 3. Clearly, the band structures in figure 3 are very alike, yet, they do give rise to rather different Kerr spectra. When considering the total DOS, one recognizes that, in

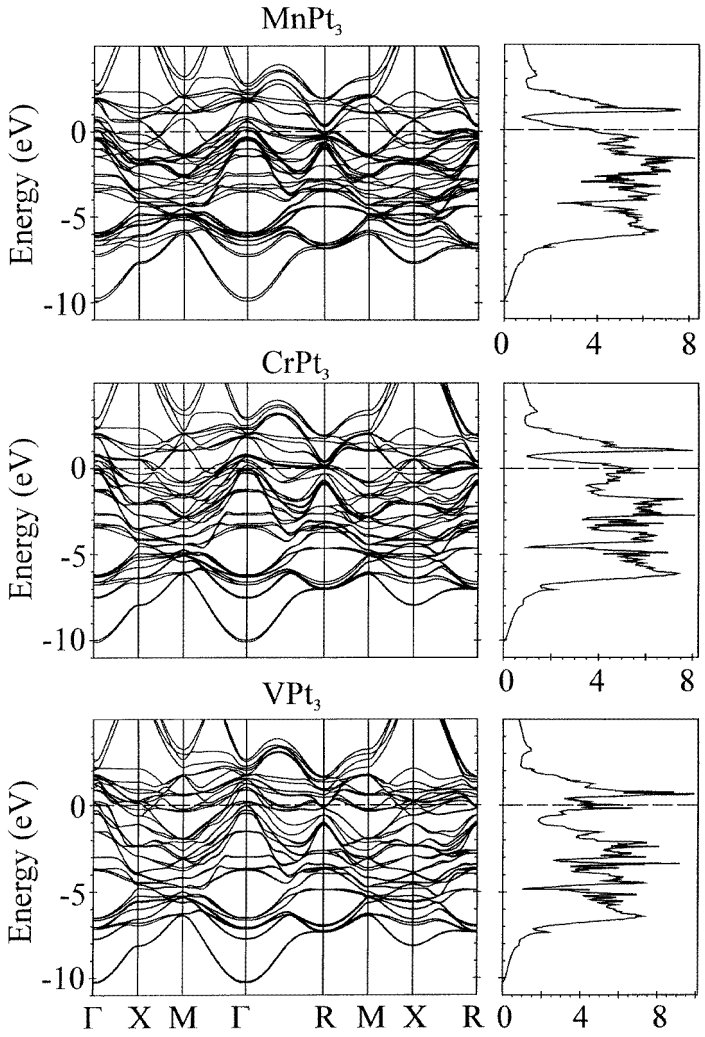

Figure 3. Continued.

particular, those of $CrPt_3$, $MnPt_3$ and $FePt_3$ are very similar. In going from $CrPt_3$ to $MnPt_3$, to $FePt_3$, the Fermi level is simply shifted upwards by filling the bands with one electron more. The DOS of VPt_3 and $CoPt_3$, on the other hand, look different and do not follow this picture. This structure of the DOS is, however, not reflected in the Kerr spectra. It is, of course, not a straightforward matter to understand the Kerr spectrum from the DOS, although this is sometimes attempted. In particular, besides the DOS the optical matrix elements, which impose the dipolar selection rules upon the interband optical transitions, are also important for the optical spectrum [21]. In the case of the XPt_3 compounds we find that the transition matrix elements affect the optical spectra in such a way that, for instance, the real part of the diagonal interband optical conductivity, $\mathrm{Re}[\sigma_{xx}]$, exhibits a maximum at about 2–3 eV for each of the XPt_3 compounds. Three compounds, VPt_3, $FePt_3$ and $CoPt_3$ do in addition exhibit another maximum in $\mathrm{Re}[\sigma_{xx}]$ at 0 eV. In the case of $FePt_3$ and $CoPt_3$ this local maximum at 0 eV in $\mathrm{Re}[\sigma_{xx}]$ gives rise to a somewhat smaller

Kerr rotation at small photon energies in these compounds. More importantly, we find that the shapes of the Kerr rotation spectra follow closely the shapes of the imaginary part of the off-diagonal optical conductivity, Im[σ_{xy}]. The off-diagonal optical conductivity is known to be brought about by an interplay of exchange splitting and SO interaction in the interband transitions [33]. The more relevant quantities for the MO Kerr effect are therefore the magnetic moments. In table 1 we compare the calculated magnetic moments of the XPt_3 compounds with experimental moments, as far as these are available. The magnetic moments of the XPt_3 alloys were studied experimentally through neutron-scattering experiments, in some cases twenty years ago. These experiments showed that $CoPt_3$ and $MnPt_3$ are ferromagnets [34,35], while $CrPt_3$ and VPt_3 are ferrimagnets [36–38], and $FePt_3$ is an anti-ferromagnet [22]. The calculated magnetic moments of $CoPt_3$ and $MnPt_3$ are in good agreement with experiment [34,35], and for $CrPt_3$ and VPt_3 the ferrimagnetic structure is in accordance with experiment, but the values of the moments only agree to a lesser extent. In the case of $CrPt_3$, the two neutron-scattering experiments yield rather different moments on Cr [36,37], which could be due to different form factors used in the evaluation of the moments [37]. Our calculated total moment of $CrPt_3$ corresponds very well with that of another recent calculation [39]. We further mention that very recently the spin moments of the XPt_3 series were calculated using the scalar-relativistic LAPW method [40]. The spin magnetic moments obtained by the LAPW method are also in reasonably good agreement with the present results. The relationship between the size of the magnetic moment and the Kerr rotation will be considered in section 3.

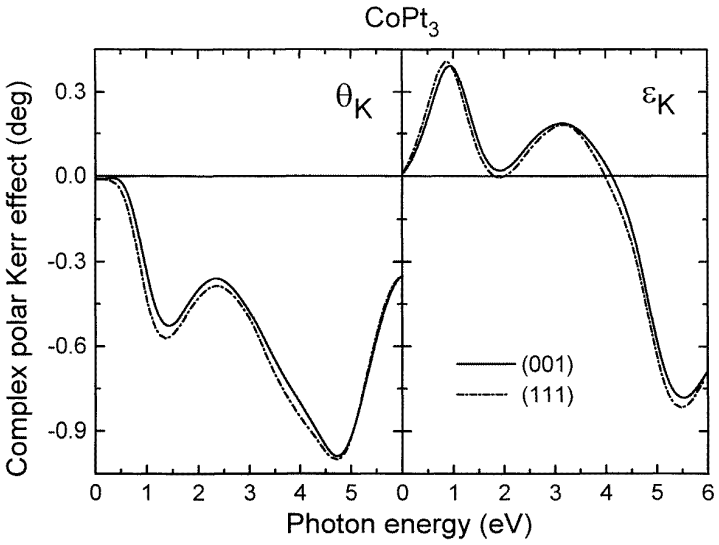

Figure 4. Dependence of the *ab initio* polar Kerr spectra of $CoPt_3$ on the magnetization axis. Theoretical polar Kerr spectra are given for the (001) and the (111) magnetization directions in the $AuCu_3$ crystal structure.

Finally, we explore the anisotropy of the Kerr spectra with respect to the magnetization axis in these compounds. The Kerr spectra of figures 1 and 2 pertain to the common magnetization orientation in these compounds, i.e., the (001) magnetization axis. A non-equivalent magnetization direction is for instance the (111) direction. In figure 4 the polar Kerr spectra of the (001) and (111) magnetization axes are shown for $CoPt_3$. The influence

of the direction of the magnetization on the Kerr spectra is clearly very small in $CoPt_3$, but it is the largest difference we found within the XPt_3 series. For this reason we do not show the orientation dependence of the other compounds. The comparatively small dependence of the Kerr spectra on the magnetization direction is undoubtedly related to the high degree of isotropy inherent to the cubic $AuCu_3$ structure. Recently we found a sizeable anisotropy effect in the Kerr spectra of some layered XPt compounds, which consist of alternating X and Pt mono-layers, and thus have a very anisotropic structure [19].

Table 1. Calculated and experimental moments of the XPt_3 (with X = V, Cr, Mn, Fe and Co) compounds. The theoretical moments have been calculated for the ferromagnetic state of the XPt_3 compounds in the $AuCu_3$ crystal structure. Spin moments are denoted by M^s, orbital moments by M^ℓ. All moments are given in Bohr magnetons (μ_B).

X	M^s_X	M^ℓ_X	M^s_{Pt}	M^ℓ_{Pt}	$M^{exp.}_X$	$M^{exp.}_{Pt}$
V	1.49	0.02	−0.05	−0.03	1.0[a]	−0.3[a]
Cr	2.73	0.16	−0.04	−0.05	2.33 ± 0.10[b]	−0.27 ± 0.05[b]
					3.37[c]	−0.26[c]
Mn	3.71	0.03	0.12	0.00	3.60 ±0.09[d]	0.17 ± 0.04[d]
Fe	3.00	0.11	0.32	0.06	—	—
Co	1.66	0.05	0.26	0.05	1.64 ± 0.04[e]	0.26 ± 0.02[e]

[a] Reference [38].
[b] Reference [36].
[c] Reference [37].
[d] Reference [35].
[e] Reference [34].

3. Discussion and conclusions

Density-functional theory in the local approximation predicts a large Kerr effect in the XPt_3 alloys. Noticeably, the Kerr rotations predicted are much larger than those calculated for e.g. Fe, Co, or Ni, where the same broadening parameter of 0.4 eV was used [14]. An important issue is therefore to identify the origin of the large Kerr effect in these compounds. To this end, we examine the dependence of the MO spectra on the exchange splitting, the SO interaction, and the optical transition matrix elements. As it can be expected that the Kerr effect in each of these compounds is of the same origin, we do this for only one compound, $CrPt_3$. The exchange splitting and the SO coupling are studied by scaling the corresponding terms in the Hamiltonian artificially with a constant prefactor. This is done in a non-self-consistent way, i.e., after self-consistency has been achieved, only one iteration is performed with the modified Hamiltonian (a self-consistent calculation would lead to a different band structure). From the resulting band structure the optical spectra are then computed. These modifications can in addition be done atom dependent, i.e., within each atomic sphere, so that we can investigate the separate effects of these quantities on Cr and on Pt. The outcomes of these model calculations for the Kerr rotation of $CrPt_3$ are shown in figure 5. In the upper panel, the importance of the exchange splitting is illustrated. When the exchange splitting on Pt is set to zero, the Kerr rotation remains as it is. But when we do the same for the exchange splitting on Cr, the Kerr rotation totally vanishes. This implies that the exchange splitting due to Cr is crucial for the sizeable Kerr rotation, but that of Pt is unimportant. Furthermore, an enhancement of the exchange splitting on Cr by a factor of two (dashed line) leads to a much larger peak in the Kerr rotation. The

middle panel of figure 5 shows the dependence on the SO coupling. If we set the SO coupling on Cr to zero, the Kerr rotation does not change (dotted line). On the other hand, when the SO coupling on Pt is zero, the Kerr rotation almost disappears (dashed line). Thus, the SO coupling of Pt is equally responsible for the large Kerr rotation as is the exchange splitting of Cr. An intermediate scaling of the SO coupling of Pt by a factor of 0.5 leads to an approximately half as large Kerr angle, thereby illustrating the almost linear dependence of the Kerr effect on the SO interaction of Pt in these compounds. The lower panel in figure 5, finally, displays the importance of the site-dependent matrix elements. Within an atomic sphere about either one of the atomic positions, the optical transition matrix elements are set to zero. If this is done for the matrix elements on Cr, the Kerr rotation does not change much. But if the matrix elements on Pt vanish, a large impact on the Kerr rotation is found (dashed curve). This indicates that the matrix elements on the Pt site are more important for bringing about the large Kerr peak at 1 eV, than are those of Cr. Making the matrix elements zero gives only an impression of which site the main contribution comes from. To obtain information about the bands that are responsible for the Kerr peak, it is instructive to exclude a particular transition matrix element. Due to the selection rules for optical transitions, these transitions can only take place between band states with an angular momentum difference of ± 1 (see e.g. Reim and Schoenes [21]). By excluding for instance the p–d transition matrix element we can investigate the contribution of this type of transition. However, as the transition matrix must be Hermitian, we have to exclude also the conjugated transition, i.e., both p–d and d–p transitions. The results of an investigation of the importance of the various transitions on Pt are shown in figure 6, for the real part of the diagonal optical conductivity, $\mathrm{Re}[\sigma_{xx}]$, the imaginary part of the off-diagonal conductivity, $\mathrm{Im}[\sigma_{xy}]$, and the Kerr rotation. The upper and middle panel of figure 6 show that both $\mathrm{Re}[\sigma_{xx}]$ and $\mathrm{Im}[\sigma_{xy}]$ are strongly reduced when the p–d and d–p interband transitions are excluded, more than when the d–f and f–d transitions are excluded. In particular the off-diagonal conductivity almost disappears in the energy region around 1 eV if the p–d and d–p transitions on the Pt sites are excluded. Because this peak in the off-diagonal conductivity at 1 eV is responsible for the peak in the Kerr rotation spectrum, this shows that the d–p and p–d transition matrix elements on Pt account for most of the Kerr effect in this frequency region. The other transitions, s–p and d–f, also have a minor influence, but excluding these still gives approximately the same Kerr rotation (see figure 6, lower panel). Thus, we conclude that the hybridized d orbitals of Pt, being subject to the strong SO interaction on the Pt site, contribute most to the optical transitions that lead to a large Kerr angle.

From these investigations the following picture of the Kerr effect in these compounds emerges: Pt is the magneto-optically active element, and creates the large Kerr rotation through its large SO interaction. The important MO transitions are the p–d and d–p transitions on Pt. The 3d elements are magneto-optically not very active. Their role is to supply through their exchange splitting enough hybridized spin-split energy bands. This understanding suggests the following recipe for finding a material having a sizeable Kerr rotation: such a material should contain elements with a large SO coupling, for instance Pt, Bi, or an actinide. Also it should contain an element having a sufficiently large magnetic moment, but this element does not need to have a strong SO interaction, such as for instance Mn. Also there should be a substantial hybridization between the valence orbitals of these two kinds of constituents. Elements which have a large, but local atomic moment, like some of the 4f elements, are in the latter respect not suited. The unhybridized, localized 4f states do not contribute much to the optical spectra, because the corresponding transition matrix elements are quite small [41]. Also, due to the lack of hybridization, other band states do

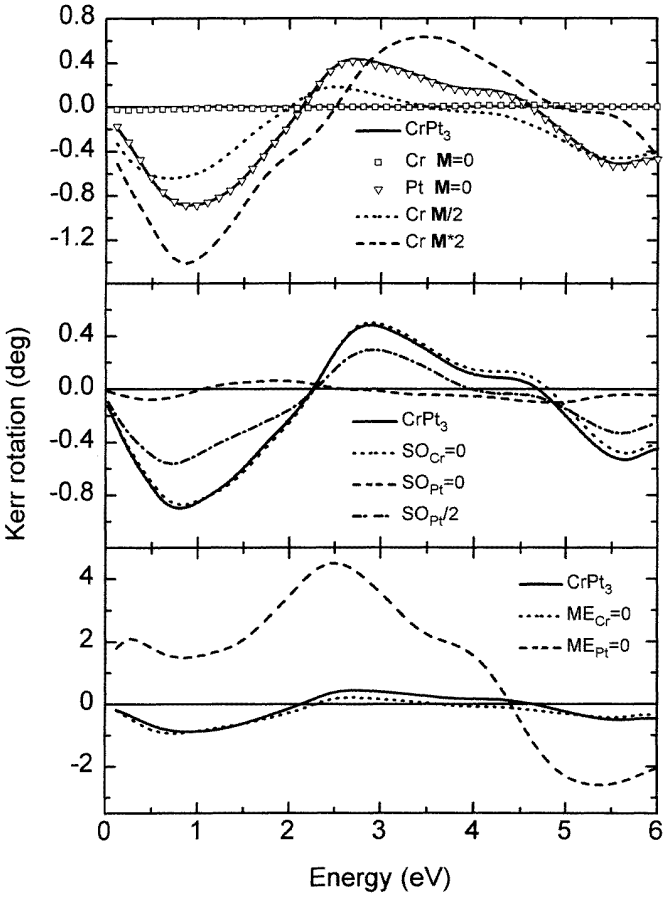

Figure 5. Study of the influence of the exchange splitting (**M**), spin–orbit (SO) coupling, and optical transition matrix elements (ME) on the Kerr rotation of $CrPt_3$. The upper panel shows the effect of multiplying the spin-polarized part of the Dirac Hamiltonian with a constant factor, on the Cr site or on the Pt site. The middle panel shows the efffect of multiplying the SO-coupling part of the Hamiltonian on Cr or on Pt with a constant prefactor (see text). The lower panel depicts the effect of setting the matrix elements on Cr or on Pt to zero.

not become sufficiently polarized, and do therefore also not contribute much [41].

The behaviour of the magnitude of the peak in the Kerr rotation spectra with respect to the 3d element, as shown in figures 1 and 2, and also the dependence of the magnitude of the Kerr effect on the magnetization, can furthermore be understood on the basis of these model calculations. The increase of the peak in the Kerr angle at about 1 eV when going from VPt_3 to $MnPt_3$ (see figure 1) is caused by the corresponding increase of the exchange splitting, as is witnessed by the magnetic moments in table 1. This is most clearly demonstrated by the scaling of the peak in the Kerr rotation of $CrPt_3$ with respect to the scaling of the exchange splitting (figure 5, upper panel). Also it can be understood from this behaviour that a reduction of the magnetization at room temperature leads to a reduction of the Kerr rotation, as was proposed for $CoPt_3$ [32]. This dependence on the magnetization also explains why the Kerr rotation of $FePt_3$ is larger than that of $CoPt_3$.

In conclusion, the series of XPt_3 compounds is predicted to exhibit rather large Kerr

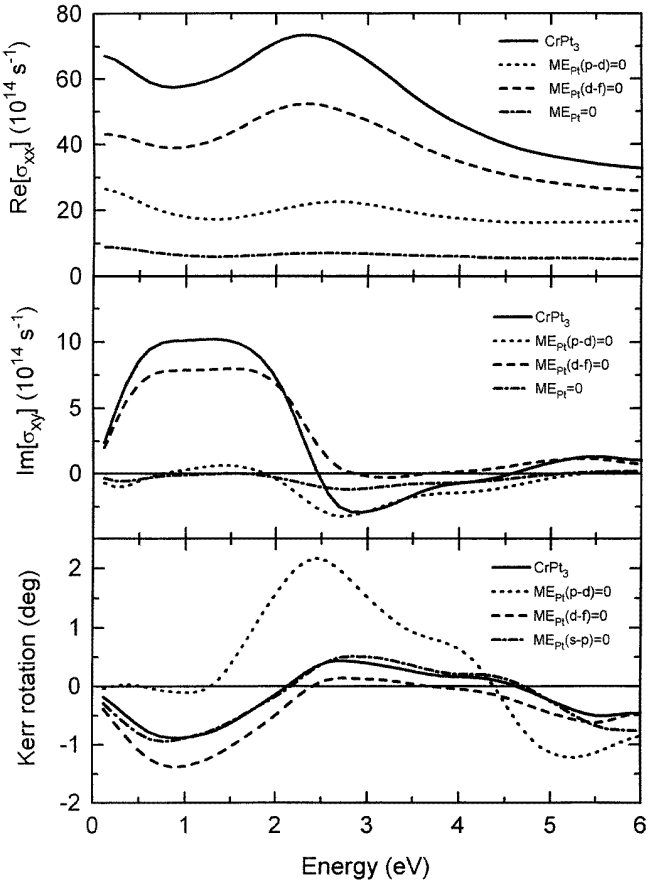

Figure 6. Influence of the exclusion of various optical matrix elements on the Pt site on the real part of the diagonal optical conductivity, Re[σ_{xx}], the imaginary part of the off-diagonal optical conductivity, Im[σ_{xy}], and the Kerr rotation. The notation ME_{Pt}(p–d) = 0 means that on the Pt site the p–d interband transitions and the d–p interband transitions are excluded from the optical matrix element.

effects. The origin of the Kerr effects is shown to be an interplay between the exchange splitting of the 3d element and the SO coupling of Pt in the hybridized bands. The dependence of the Kerr spectra in the XPt_3 compounds on the crystallographic direction of the magnetization is found to be very small. This finding agrees with the high degree of isotropy of the cubic $AuCu_3$ crystal structure. The agreement between the *ab initio* calculated Kerr spectra and the experimental result for $MnPt_3$ [7,8], finally, looks very promising. Further measurements on these compounds are desirable and needed, in order to obtain a complete picture of the correspondence between experimental and first-principles Kerr spectra.

Acknowledgments

We thank Dr S Iwata for sending us the experimental Kerr spectra of $MnPt_3$. This work was supported financially by a grant from the State of Saxony under project No 4-7541.83-

MP2/301. VNA gratefully acknowledges support from the G Soros Foundation under Contract No U 42000 (Support for basic Sciences in the former Soviet Union).

References

[1] van Engen P G, Buschow K H J, Jongebreur R and Erman M 1983 *Appl. Phys. Lett*. **42** 202
[2] Lairson B M and Clemens B M 1993 *Appl. Phys. Lett*. **63** 1438
[3] Harp G R, Weller D, Rabedeau T A, Farrow R F C and Toney M F 1993 *Phys. Rev. Lett*. **71** 2493
[4] Zeper W B, Greidanus F J A M, Garcia P F and Fincher C R 1989 *J. Appl. Phys*. **65** 4971
[5] Weller D, Brändle H, Gorman G, Lin C-J and Notarys H 1992 *Appl. Phys. Lett*. **61** 2726
[6] Sato K, Ikedame H, Tosaka Y, Tsuzukiyama K, Togami Y and Fujisawa M 1993 *J. Magn. Magn. Mater*. **126** 572
[7] Kato T, Kikuzawa H, Iwata S, Tsunashima S and Uchiyama S 1995 *J. Magn. Magn. Mater*. **140–144** 713
[8] Kato T, Iwata S, Tsunashima S and Uchiyama S 1995 *J. Magn. Soc. Japan* **19** 205
[9] Kubo R 1957 *J. Phys. Soc. Japan* **12** 570
[10] Wang C S and Callaway J 1974 *Phys. Rev*. B **9** 4897
[11] Hohenberg P and Kohn W 1964 *Phys. Rev*. B **136** 864
[12] Kohn W and Sham L 1965 *Phys. Rev*. A **140** 1133
[13] von Barth U and Hedin L 1972 *J. Phys. C: Solid State Phys*. **5** 1629
[14] Oppeneer P M, Maurer T, Sticht J and Kübler J 1992 *Phys. Rev*. B **45** 10924
[15] Osterloh I, Oppeneer P M, Sticht J and Kübler J 1994 *J. Phys. Condens. Matter* **6** 285
[16] Oppeneer P M, Antonov V N, Kraft T, Eschrig H, Yaresko A N and Perlov A Ya 1995 *Solid State Commun*. **94** 255
[17] Guo G Y and Ebert H 1995 *Phys. Rev*. B **51** 12633
[18] Uspenskii Y A, Kulatov E T and Halilov S V 1995 *Sov. Phys.–JETP* **80** 952
[19] Oppeneer P M, Kraft T, Antonov V N and Eschrig H to be published
[20] Cebollada A, Weller D, Sticht J, Harp G R, Farrow R F C, Marks R F, Savoy R and Scott J C 1994 *Phys. Rev*. B **50** 3419
[21] Reim W and Schoenes J 1990 *Ferromagnetic Materials* Vol 5 ed K H J Buschow and E P Wohlfarth (Amsterdam: North-Holland) p 133
[22] Bacon G E and Crangle J 1963 *Proc. R. Soc. (London)* A **272** 387
[23] Erskine J L and Stern E A 1975 *Phys. Rev*. B **12** 5016
[24] Williams A R, Kübler J and Gelatt C D 1979 *Phys. Rev*. B **19** 6094
[25] Nemoshkalenko V V, Krasovskii A E, Antonov V N, Antonov Vl N, Fleck U, Wonn H and Ziesche P 1983 *Phys. Status Solidi (b)* **120** 283
[26] Andersen O K 1975 *Phys. Rev*. B **12** 3060
[27] Antonov V N, Bagljuk A I, Perlov A Ya, Nemoshkalenko V V, Antonov Vl N, Andersen O K and Jepsen O 1993 *Low Temp. Phys*. **19** 494
[28] Kaburagi M, Tonegawa T and Ebina K 1990 *J. Magn. Magn. Mater*. **90–91** 161
[29] Villars P and Calvert L D 1985 *Pearson's Handbook of Crystallographic Data for Intermetallic Phases*, (American Society for Metals, Metals Park)
[30] Krinchik G S and Artem'ev V A 1968 *Sov. Phys.–JETP* **26** 1080
[31] Buschow K H J, van Engen P G and Jongebreur R 1983 *J. Magn. Magn. Mater*. **38** 1
[32] Weller D, Sticht J, Harp G R, Farrow R F C and Brändle H 1993 *Magnetic Ultrathin Films: Multilayers and Surfaces/Interfaces and Characterization (Mat. Res. Soc. Symp. Proc. No 313)* ed B T Jonker (Pittsburgh: Materials Research Society) p 501
[33] Argyres P N 1955 *Phys. Rev*. **97** 334
[34] Menzinger F and Paoletti A 1966 *Phys. Rev*. **143** 365
[35] Pickart S J and Nathans R 1962 *J. Appl. Phys*. **33** S1336
[36] Pickart S J and Nathans R 1963 *J. Appl. Phys*. **34** 1203
[37] Burke S K, Rainford B D, Williams D E G, Brown P J and Hukin D A 1980 *J. Magn. Magn. Mater*. **15–18** 505
[38] Kawakami M and Goto T 1979 *J. Phys. Soc. Japan* **46** 1492
[39] Lu Z W, Klein B M and Zunger A 1995 *Phys. Rev. Lett*. **75** 1320
[40] Shirai M, Maeshima H and Suzuki N 1995 *J. Magn. Magn. Mater*. **140–144** 105
[41] Oppeneer P M 1995 unpublished